INDUCED PRESSURE-VARIATION TRANSPORT IN UNCONFINED AQUIFER

Jet-Chau Wen* Kuo-Shun Huang
Research Center of Soil & Water Resources and Natural Disaster Prevention
National Yunlin University of Science and Technology
Yunlin, Taiwan 640, R.O.C.

Horng-Guang Leu
Bureau of Solid Waste Management, Environmental Protection Administration
Government of Republic of China
Taipei, Taiwan 100, R.O.C.

Key Words: head potential fluctuation, propagation, aquifer.

ABSTRACT

The purpose of this study is to develop a numerical model and simulate the behavior of the head potential fluctuation in subsurface flows. Numerical and analytical solutions are presented. Impacts of storativity and porosity on the head potential fluctuation are investigated in this paper. It is found, in one-dimensional subsurface flows, that porosity and storativity play an important role in the propagation of the head potential fluctuation. In addition, an asymptotic behavior of the head potential fluctuation is not reached until the head propagation travels more than three-fourths of the total length of the aquifer.

I. INTRODUCTION

The stochastic process has been used in the hydrological analysis of heterogeneous subsurface parameters for two decades. Spectral-density theory and method of perturbations were applied to stochastic approaches to differential equations with stochastic input parameters to derive the solutions of subsurface problems (Gelhar, 1974; Bakr, 1976; Gelhar, 1976; Bakr *et al*., 1978; Gujtahar *et al*., 1978; Gelhar, 1986; Marschall and Barczewski, 1989). Most research stemmed from the spectrum of lognormal distribution of hydraulic conductivity (Bakr, 1976; Gelhar, 1976; Bakr *et al*., 1978; Gujtahar *et al*., 1978; Gelhar, 1986). In 1994, Hantush and Mariño presented an examination of the hydraulic head variation in a confined aquifer. They investigated the behavior of the hydraulic head with the second moment of the head fluctuation. In Hantush and Mariño's (1994) study, they described the head variance of a confined aquifer in terms of the space and time domain by using a numerical method (finite element approach).

For temporal variables of subsurface flows, the variation of groundwater level in an unconfined aquifer may change at monthly (or seasonal) frequencies. It is common to focus on the quasi-steady-state of the variation rather than to explore its detailed unsteady response (Gelhar, 1993). However, the dynamic response of subsurface-flow systems may have a significant amount of information about the nature of the flow system. This motivates us to investigate the impact of the subsurface parameters on the flow system in an unconfined aquifer.

*Correspondence addressee, who is also affiliated with the Department of Environmental and Safety Engineering, National Yunlin University of Science and Technology.

A numerical simulation of the finite element method to obtain the impact of the subsurface parameters is applied in this paper. Two one-dimensional subsurface phreatic aquifer systems will be investigated. The stochastic input parameters are the water tables of the subsurface and the free surface (which fluctuates) of a stream merging with the aquifer. The other input parameters are transmissivity (or hydraulic conductivity) and porosity which are treated in deterministics.

One of these two phreatic aquifer systems is the same as the one in Gelhar (1974), which will be compared to our numerical results. His case considers the water table propagation of a subsurface horizontal aquifer due to the fluctuation of its merging stream (a constant head boundary condition). Normalized spectral-density function of the head potential will be applied to obtain the fluctuation behavior of the head potential of the subsurface.

For the other system, the second case, a vertical flow system will be examined by both analytical and numerical methods. Two examples will be given to represent two different vertical aquifer properties in order to show their effects on the head potential fluctuation.

II. MATHEMATICAL DEVELOPMENT

The continuity equation in a general form for unsteady-state subsurface flows can be described as (Bear, 1972)

$$S_s\frac{\partial h}{\partial t} = K\nabla^2 h + q \tag{1}$$

where

- S_s denotes the specific storativity of the aquifer [1/length];
- K represents the hydraulic conductivity of the aquifer [length/time];
- ∇^2 is the Laplace operator;
- h denotes the Hubbert's potential head (a function of position and time) of the aquifer [length];
- t is the time variable [time];
- q represents sink or source term in the aquifer [1/time].

In Eq. (1), the specific storativity (S_s) is used for groundwater flow with the consideration of vertical flow (parallel to the gravitational direction). However, if we only consider the horizontal flow (normal to the gravitational direction), the S_s in Eq. (1) can be changed to the storativity (s) only due to the integration along the depth of the aquifer (parallel to the gravitational direction) (Bear, 1972).

The boundary conditions are three types in general for Eq. (1) and are written as:

1. Potential boundary condition:

$$h(\Gamma)=H(t) \tag{2}$$

2. No-flow boundary condition:

$$\frac{\partial}{\partial n}h(\Gamma_1) = 0 \tag{3}$$

3. Linear free-surface boundary condition:

$$K\frac{\partial h}{\partial n} + n_0\frac{\partial h}{\partial t} = \varepsilon \tag{4}$$

where

- n_0 represents the effective porosity of a phreatic aquifer [dimensionless];
- ε represents the infiltration rate in the phreatic aquifer [length/time];
- Γ denotes the interface boundary between the phreatic aquifer and a merging stream;
- Γ_1 represents the phreatic aquifer boundary, not including the interface boundary (Γ);
- $H(t)$ denotes the river stage (a function of time) or the driving head potential affecting the free surface of the aquifer [length].

1. Stochastic Differential Equation for Transient Flow in Phreatic Aquifer—Cross-Sectional Model

By using the first-order method of perturbations for the potential and singular terms, h and q are described as

$$h(\vec{x}, t) = \overline{h}(\vec{x}) + h'(\vec{x}, t) \text{ and}$$

$$q(\vec{x}, t) = \overline{q}(\vec{x}) + q'(\vec{x}, t) \tag{5}$$

where

$\overline{h}$ and $\overline{q}$ are the means of h and q, respectively [$\overline{h}$: length; $\overline{q}$: 1/time];

h' and q' are the perturbations of h and q, respectively [h': length; q': 1/time];

$\vec{x}$ represents a position vector [length].

Substituting Eq. (5) into Eq.(1) leads to

$$S_s\frac{\partial \overline{h}}{\partial t} + S_s\frac{\partial h'}{\partial t} = K\nabla^2\overline{h} + K\nabla^2 h' + \overline{q} + q' \tag{6}$$

Since the perturbations of h and q have zero means, Eq. (6) is rewritten by taking the mean of it as

$$S_s\frac{\partial \overline{h}}{\partial t} = K\nabla^2\overline{h} + \overline{q} \tag{7}$$

Then, subtracting Eq. (7) from Eq. (6) leads to

$$S_s\frac{\partial h'}{\partial t} = K\nabla^2 h' + q' \tag{8}$$

The result, Eq. (8), is known as the stochastic differential equation of the continuity equation.

Using the Fourier-Stieltjes Transform for these perturbations of h and q leads to

$$h'(x, y, t) = \int_{-\infty}^{\infty} \exp(i\,\omega t)dZ_h(x, y, \omega) \text{ and}$$

$$q'(x, y, t) = \int_{-\infty}^{\infty} \exp(i\,\omega t)dZ_q(x, y, \omega) \tag{9}$$

where ω denotes the frequency and t represents the time variable.

Substituting Eq. (9) into Eq. (8), a generalized amplitude equation is obtained,

$$\nabla(K\nabla dZ_h) - S_s\omega i dZ_h + dZ_q = 0 \tag{10}$$

where dZ represents a complex Fourier amplitude that can be expressed in terms of real and imaginary parts:

$$dZ_h = \phi_r + i\phi_i \text{ and } dZ_q = \psi_r + i\psi_i \tag{11}$$

where ϕ_r and ϕ_i are the real and imaginary parts, respectively, of dZ_h; ψ_r and ψ_i are the real and imaginary parts, respectively, of dZ_q.

Replacing Eq. (11) with Eq. (10), we obtain two equations, one for the real part and the other for the imaginary part of the Fourier amplitude (dZ_h):

$$\nabla(K\nabla\phi_r) + S_s\omega\phi_i + \psi_r = 0 \tag{12}$$

and

$$\nabla(K\nabla\phi_i) - S_s\omega\phi_r + \psi_i = 0 \tag{13}$$

These two equations have to be simultaneously solved, corresponding to their appropriate boundary conditions. The boundary conditions shown in Eqs. (2), (3), and (4), therefore, need to be transformed into a frequency domain.

In most cases, the solutions of Eqs. (12) and (13) require a numerical method. In this study, we apply the finite element method to solve these two equations in a two-dimensional formula.

2. Finite-Element Approximation

The standard quadrilateral element of the finite element method is used for this study (Zienkiewicz and Taylor, 1989). The approximation of ϕ_r, ϕ_i and ψ_r, ψ_i of each element is expressed in general as

$$f(x, y) \cong \sum_{i=1}^{Ne} N_i(x, y)f_i \tag{14}$$

where

$N_i(x, y)$ denotes the interpolation function corresponding to node i;
f_i represents the value of function $f(x,y)$ at node i;
$f(x, y)$ represents any one of ϕ_r, ϕ_i, ψ_r, or ψ_i;
N_e is the total number of nodes at an element.

Applying the weighted residual method (Zienkiewicz and Taylor, 1989) to Eq. (12), using the appropriate boundary conditions, and then dividing the aquifer domain into many standard quadrilateral elements, we obtain a set of equations for all of the elements,

$$[A]\{\phi_r\} + [B]\{\phi_i\} = \{C\} \tag{15}$$

where

$$[A] = A_{ij} = \iint_{\Omega} K\left(\frac{\partial N_i}{\partial x}\frac{\partial N_j}{\partial x} + \frac{\partial N_i}{\partial y}\frac{\partial N_j}{\partial y}\right)d\Omega;$$

$$[B] = B_{ij} = \iint_{\Omega} S_s\omega N_i N_j d\Omega + \int_{\Lambda} n\omega N_i N_j d\Lambda;$$

$$\{C\} = C_i = -\sum_j \int_{\Lambda} N_i N_j \varepsilon_r d\Lambda - \iint_{\Omega} N_i \psi_r d\Omega;$$

Λ denotes the boundary of an aquifer;
Ω represents the domain of an aquifer;
$\int_{\Lambda} \cdots d\Lambda$ denotes the integral of the elements at the free surface of the aquifer;
$\iint_{\Omega} \cdots d\Omega$ represents a double integral of elements in the aquifer domain.

Similarly, for Eq. (13) we obtain

$$[D]\{\phi_r\} + [E]\{\phi_i\} = \{F\} \tag{16}$$

where

$$[D] = D_{ij} = -B_{ij};$$

$$[E] = E_{ij} = A_{ij};$$

$$[F] = F_i = -\sum_j \int_{\Lambda} N_i N_j \varepsilon_r d\Lambda - \iint_{\Omega} N_i \psi_i d\Omega$$

Therefore, from Eqs. (15) and (16), a program for this finite-element approximation can be completed.

III. CASE STUDIES: ONE-DIMENSIONAL FLOW PROBLEMS

1. Horizontal Flow Case

In this case, we consider a phreatic aquifer with an impervious bottom, which merges with a stream. Because it is parallel to the river from a plane viewpoint (as shown in Fig. 1), this problem can be reduced to a one-dimensional problem by adopting the Dupuit assumption (Bear, 1972). This case is the same as the case presented in Gelhar (1974). In his paper, (Gelhar, 1974) he presented the analytical solution of the head spectrum. However, he did not give the numerical solution during his research. Therefore, the motivation of this problem is to check the numerical program set up in the last section to see whether it works for the horizontal flow case.

The saturated thickness of this phreatic aquifer is assumed to be constant. Consequently, the transmissivity is dealt with as a constant when the hydraulic conductivity is assumed to be homogeneous in the entire aquifer. The governing equation for this horizontal flow problem is described as ($|h-h_0|<<h_0$, where h_0 represents the river stage)

$$s\frac{\partial h}{\partial t} = T\frac{\partial^2 h}{\partial x^2} \tag{17}$$

where

- $h=h(x,t)$ represents the Hubbert's potential in the phreatic aquifer [length];
- x denotes the horizontal position [length];
- s is the aquifer storativity [dimensionless];
- T denotes the transmissivity [length^2/time].

In addition, the boundary conditions for Eq. (17) can be expressed as

$$x=0,\ \ h=h_0$$

and

$$x=L,\ \frac{\partial h}{\partial x} = 0 \tag{18}$$

where L denotes the aquifer total length in a horizontal direction.

Using the same procedure as used in the stochastic differential equation for transient flows, Eqs. (8)-(10), an ordinary differential equation of the amplitude equation for head perturbations is obtained,

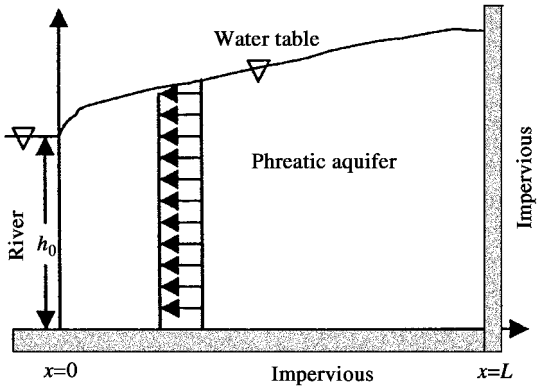

Fig. 1 One-dimensional horizontal flow case in a phreatic aquifer (in steady state)

$$Td''Z_h-(i\omega s)dZ_h= 0 \tag{19}$$

The transformed boundary conditions for Eq. (19) are

$$x=0,\ \ h'=h_0',\ \ dZ_h=dZ_H$$

and

$$x=L,\ \frac{\partial h'}{\partial x} = 0\ ,\ \frac{d(dZ_h)}{dx} = 0 \tag{20}$$

Since ω is valid in the range of $(-\infty, \infty)$, Eq. (19) has to be solved for $\omega\geq 0$, and $\omega<0$ as

$$dZ_h=F(\omega, x)dZ_H \tag{21}$$

where $F(\omega, x)=\dfrac{\cos h[b(x-L)]}{\cos h(bL)}$, and $b=\sqrt{\dfrac{|\omega|s}{2T}}$ (1+i).

Using the spectral theorem (Gelhar, 1993), the spectrums of the head potential in the aquifer and at the riverside are

$$E[dZ_h\ \ dZ_h^*] = S_{hh}d\omega\ ,$$

and

$$E[dZ_H\ \ dZ_H^*] = S_{HH}d\omega\ ,$$

where

- dZ_h^* and dZ_H^* represent the conjugate function of dZ_h and dZ_H, respectively;
- S_{hh} represents the spectrum of the head potential in the unconfined aquifer;
- S_{HH} denotes the spectrum of the head potential at the riverside (x=0);
- $d\omega$ represents the differential of the frequency.

Then, if we again use the spectral theorem by

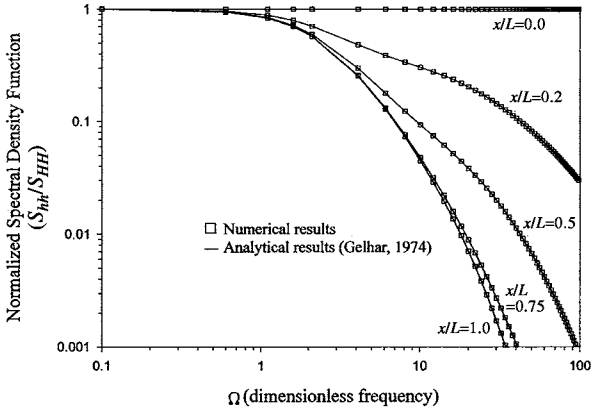

Fig. 2 Solutions of the horizontal flow case

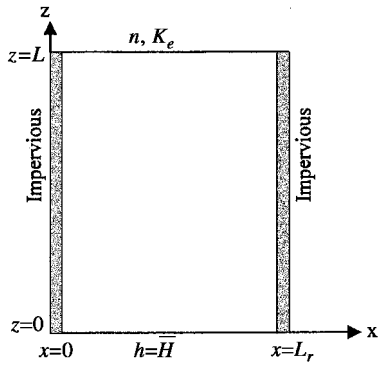

Fig. 3 One-dimensional vertical flow case in a phreatic aquifer (in steady state)

conjugating Eq. (21) and then multiply the conjugate of Eq. (21) by Eq. (21), it leads to

$$E[dZ_h \; dZ_h^*] = FF^* E[dZ_H \; dZ_H^*]$$

and

$$S_{hh}=FF^*S_{HH} \tag{22}$$

where F^* is the conjugate function of F. We can, therefore, define a normalized spectral-density function of the head potential, S_{hh}/S_{HH}, as

$$\frac{S_{hh}}{S_{HH}} = FF^* = \frac{\cos h[2(\frac{\Omega}{2})^{0.5}(\frac{x}{L}-1)] + \cos[2(\frac{\Omega}{2})^{0.5}(\frac{x}{L}-1)]}{\cos h[2(\frac{\Omega}{2})^{0.5}] + \cos[2(\frac{\Omega}{2})^{0.5}]} \tag{23}$$

where $\Omega=\omega\times L\times L\times s/T$. Therefore, Eq. (23) represents the normalized spectral-density function of Hubbert's potential in this horizontal flow case. Then, in order to compare the numerical result of the finite-element approximation to the analytical one of Eq. (23), we need to assign values to the input parameters (L, T, and s) as

L=5000 ft, T=10000 ft^2/year, s=0.002

Figure 2 depicts the results of the finite-element approximation and of Eq. (23).

The absolute difference between the result of the finite-element approximation and of the analytical solution (Eq. 23) is less than 10^{-4}. This shows that the result of the finite-element approximation is very near to the result of the analytical solution, which is the same as Gelhar's (1974). The normalized spectral-density function of the Hubbert's potential in this aquifer is found to decrease as the dimensionless frequency increases under fixed distance from the river circumstances. It is apparent that the fluctuation of the Hubbert's potential in this aquifer is influenced by the river stage. Therefore, the spectral-density function of the Hubbert's potential at the riverside is equal to the spectral-density function of the river stage and then decreases quickly at the greatest distance from the riverside. Eventually, the fluctuation of the Hubbert's potential in this aquifer becomes approximately zero at the impervious boundary ($x=L$).

Another finding is that the perturbation of the Hubbert's potential is almost the same as the one at the farthermost boundary from the river when the distance in the aquifer from the river is greater than three-fourths of the length of the aquifer. In other words, when the distance in the aquifer from the river is greater than three-fourths of the length of the aquifer, this fluctuation reaches its asymptotic value.

2. Vertical Flow Case

Considering a phreatic aquifer not only with a leaking bottom at $z=0$ but with the surrounding vertical impervious layers at $x=0$ and $x=L$, groundwater can, therefore, move in the vertical direction only, as shown in Fig. 3. The source of the perturbation comes from the head fluctuation at the leakage boundary (at $z=0$).

Thus, the governing equation for this problem can be expressed as

$$\frac{\partial}{\partial z}(K\frac{\partial h}{\partial z}) = S_s\frac{\partial h}{\partial t} \tag{24}$$

and the boundary conditions as

$$z=0,\; h(t)=H(t)$$

and

$$z=L,\; K\frac{\partial h}{\partial z} + n\frac{\partial h}{\partial t} = 0 \tag{25}$$

where n represents the effective porosity at the water table, and S_s denotes the specific storativity for a saturated zone.

Before we start to use the first-order method of perturbation for solving the problem, we would like to explain the first-order perturbation for the boundary conditions. In Eq. (25), we assume that the water table in the unconfined aquifer during the steady state is at $z=L$. In other words, the head potential at $z=0$ during the steady state is $h=\overline{H}$ (or say $\overline{H}$ is the mean head potential at $z=0$). The $\overline{H}$ is a constant. Then, we allow the first-order small perturbation of the head potential to come into the unconfined system. It leads to, at $z=0$,

$$h(t)=\overline{H}+H'(t)$$

where $H'(t)$ represents the first-order small perturbation of the head potential at $z=0$. Since the head potential at $z=0$ has a small perturbation, it will propagate through the aquifer and reach, namely, the upper boundary at $z=L$. Therefore, the head potential at $z=L$ will become

$$h(t)=\overline{h}+h'(t)$$

where $\overline{h}$ denotes the mean head potential at $z=L$; $h'(t)$ represents the small fluctuation of the head potential at $z=L$.

Then the boundary condition at $z=L$ can be written as

$$K\frac{\partial(h')}{\partial z}+n\frac{\partial(h')}{\partial t}=0$$

Assuming homogeneous soils, K = constant, and using the same derivative procedure as used for the horizontal flow case, Eqs. (8)-(10), the normalized spectral-density function of $h'(x,t)$, S_{hh}/S_{HH}, is obtained as

$$\frac{S_{hh}}{S_{HH}}=\frac{A+B-C}{D+E-F} \tag{26}$$

where

$$A=\left\{\beta\cos\left[\left(\frac{\bar{\Omega}L}{2}\right)^{1/2}\left(\frac{z}{L}-1\right)\right]+\left(\frac{\bar{\Omega}_0}{L}\right)\sin\left[\left(\frac{\bar{\Omega}L}{2}\right)^{1/2}\left(\frac{z}{L}-1\right)\right]\right\}^2$$

$$B=\left\{\beta\cosh\left[\left(\frac{\bar{\Omega}L}{2}\right)^{1/2}\left(\frac{z}{L}-1\right)\right]-\left(\frac{\bar{\Omega}_0}{L}\right)\sinh\left[\left(\frac{\bar{\Omega}L}{2}\right)^{1/2}\left(\frac{z}{L}-1\right)\right]\right\}^2$$

$$C=\beta^2\left\{\sin^2\left[\left(\frac{\bar{\Omega}L}{2}\right)^{1/2}\left(\frac{z}{L}-1\right)\right]-\sinh^2\left[\left(\frac{\bar{\Omega}L}{2}\right)^{1/2}\left(\frac{z}{L}-1\right)\right]\right\}$$

$$D=\left\{\beta\cos\left[\left(\frac{\bar{\Omega}L}{2}\right)^{1/2}\right]-\left(\frac{\bar{\Omega}_0}{L}\right)\sin\left[\left(\frac{\bar{\Omega}L}{2}\right)^{1/2}\right]\right\}^2$$

$$E=\left\{\beta\cosh\left[\left(\frac{\bar{\Omega}L}{2}\right)^{1/2}\right]+\left(\frac{\bar{\Omega}_0}{L}\right)\sinh\left[\left(\frac{\bar{\Omega}L}{2}\right)^{1/2}\right]\right\}^2$$

$$F=\beta^2\left\{\sin^2\left[\left(\frac{\bar{\Omega}L}{2}\right)^{1/2}\right]-\sinh^2\left[\left(\frac{\bar{\Omega}L}{2}\right)^{1/2}\right]\right\}$$

$$\bar{\Omega}=\frac{L|\omega|S_s}{K}$$

$$\bar{\Omega}_0=\frac{L|\omega|n}{Ke}$$

$$\beta=\sqrt{\frac{|\omega|S_s}{2K}}$$

S_{hh} represents the spectrum of the head potential fluctuation at the inner domain of the unconfined aquifer;

S_{HH} denotes the spectrum of the head potential fluctuation at the lower boundary of the unconfined aquifer ($z=0$);

Ke represents the saturated hydraulic conductivity for an unsaturated zone.

With the analytical solution Eq. (26) and the numerical approach of the finite element method, two examples involving subsurface problems will be solved in the vertical aquifer. Different values are given to the specific storativity and the effective porosity to indicate their effects on the hydraulic potential fluctuation.

The first example is

$K=Ke=10$ ft/year, $S_s=0.0001$/ft, $n=0.1$, $L=100$ ft,

at $z=0$ ft, $\overline{H}=1.0$.

Results of the analytical solution and the numerical approach for this example are illustrated in Fig. 4. The quantity of the specific storativity in the aquifer ($S_s=0.0001$/ft) is much less than the effective porosity at the free surface ($n=0.1$). In other words, the

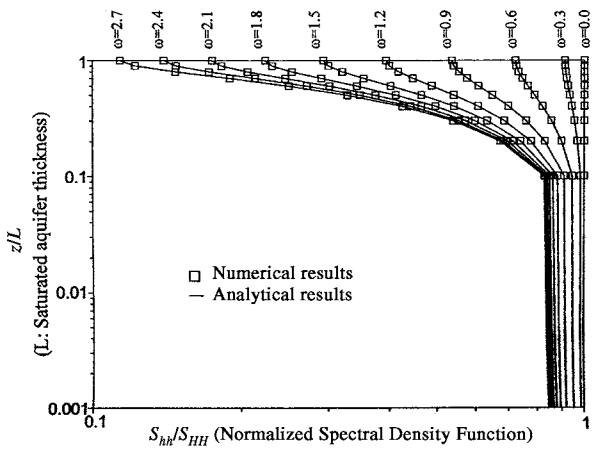

Fig. 4 Solutions of the first example in the vertical flow case (Note: *w* is the frequency of pressure fluctuation)

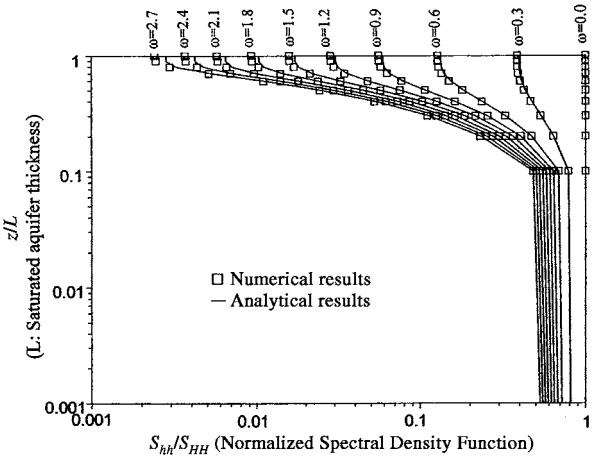

Fig. 5 Solutions of the second example in the vertical flow case (Note: *w* is the frequency of pressure fluctuation)

effect of the specific storativity on the fluctuation of the Hubbert's potential can, therefore, be observed.

It is found that the higher the elevation from the bottom of this vertical aquifer, the less the spectral-density of the Hubbert's potential. This behavior is more obvious for the larger dimensionless frequencies than for the smaller ones. Since the specific storativity (0.0001/ft) in this phreatic aquifer system is small, the fluctuation of the Hubbert's potential easily propagates from the bottom of this aquifer to the upper part of it. In turn, this fluctuation starts to decay when it reaches the free surface due to the high effective porosity, especially for higher frequencies. Again, an asymptotic behavior of the spectral-density function of the Hubbert's potential occurs when the elevation is greater than three-fourths of the height of the initial water table (*L*).

The input data for the second example are

$K=Ke$=10ft/year, S_s=0.01/ft, n=0.01, L=100ft,

at z=0 ft, $\overline{H}$ =1.0.

Results for the analytical and numerical solutions for this example are shown in Fig. 5. In this example, the specific storativity is equal to the effective porosity ($S_s=n$=0.01).

It can be seen that the fluctuation of the Hubbert's potential as it propagates from the bottom of this aquifer to the upper part is not so significant as the previous case since the specific storativity in this case is much higher than the previous one. However, the fluctuation in this example does not decay so fast as the one in the first. Also, the asymptotic behavior of the spectral-density functions of the Hubbert's potential still exists when the elevation is higher than three-fourths of the height of the aquifer.

In this case, it is apparent that the finite-element approximation has a large error at the free surface of the water table. This can be recognized in this example by viewing Fig. 5. For instance, the maximum error, which is the difference between the numerical solution and the analytical solution, occurs at the free surface ($z=L$). Specifically, the largest one occurs at the frequency ω=2.7, and its value is $|2.43\times10^{-3}-2.18\times10^{-3}|=2.5\times10^{-4}$. Because this example has a smaller effective porosity, the natural boundary conditions at the free surface become more sensitive to error. By comparing these results to those of the analytical solution, one sees that the results of the finite-element approximation are still applicable to this situation in spite of the large error at the free surface.

In conclusion, if we disregard the free surface area in Fig. 5, the finite-element approximation can be applied to both examples to investigate the fluctuation behavior of the Hubbert's potential.

IV. SUMMARY

The impact of the storativity of a phreatic aquifer on the fluctuation of Hubbert's potential was investigated in this study. For the vertical flow case only, the effective porosity was found to be an important factor at the free surface of a phreatic aquifer. The smaller the porosity, the higher the fluctuation of the Hubbert's potential.

In both horizontal and vertical aquifers, it was found that the storativity plays an important role in the pressure fluctuation propagation in the phreatic aquifer. Also in both aquifers, an asymptotic behavior of the spectral-density function of the Hubbert's potential cannot be found until the fluctuation propagates over three-fourths of the total distance.

The numerical approach of the finite-element

approximation was applied to simulate the spectral-density function of the Hubbert's potential in this study. The result showed that this finite-element approximation could predict the behavior of the fluctuation of the Hubbert's potential in a one-dimensional subsurface flow very well.

Meanwhile, we would like to emphasize again that the Dupuit assumption and small perturbation are used in this study. Therefore, in reality, the result of our study may not be applicable to the water table in an unconfined aquifer with a large head slope in a horizontal direction. Therefore, more study may have to be done in the future for large head slope cases in unconfined aquifers.

ACKNOWLEDGMENTS

National Science Council under grants NSC 88-2218-E-244-008 and NSC-83-0209-E-033-002 sponsors this work. The author would like to acknowledge Ms. Resta Saphore-Cheng who helped in writing. Also, the cooperation of Mr. I.-F. Lu and Miss C.-D. Cheng, who are working in the research center of soil & water resources and natural disaster prevention, helped in creating the figures.

NOMENCLATURE

$d\omega$	differential of frequency
dZ	a complex Fourier amplitude expressed in terms of real and imaginary parts
dZ_h^*	conjugate function of dZ_h
dZ_H^*	conjugate function of dZ_H
F^*	conjugate function of F
f_i	value of function at $f(x,y)$ at node i
$f(x,y)$	represents any one of ϕ_r, ϕ_i, ψ_r, or ψ_i
h	Hubbert's potential head (a function of position and time) of the aquifer [length]
$\overline{h}$	mean of h [length]
h'	perturbation of h [length]
$H(t)$	river stage (a function of time) or the driving head potential affecting the free surface of the aquifer [length]
$h'(t)$	small fluctuation of head potential at $z=L$
$h=h(x,t)$	Hubbert's potential in phreatic aquifer [length]
K	hydraulic conductivity of the aquifer [length/time]
Ke	saturated hydraulic conductivity for unsaturated zone
L	aquifer total length in horizontal direction
n	effective porosity of phreatic aquifer [dimensionless]
N_e	total number of nodes at an element
$N_i(x,y)$	interpolation function corresponding to node i
q	sink or source term in the aquifer [1/time]
$\overline{q}$	mean of q [1/time]
q'	perturbation of q [1/time]
s	aquifer storativity [dimensionless]
S_s	specific storativity of the aquifer [1/length]
S_{hh}	spectrum of head potential in unconfined aquifer
S_{HH}	spectrum of head potential at boundary
t	time variable [time]
T	transmissivity [length^2/time]
x	horizontal position [length]
$\vec{x}$	position vector [length]
β	constant of a variable
Γ	interface boundary between the phreatic aquifer and a merging stream
Γ_1	phreatic aquifer boundary, not including the interface boundary (Γ)
∇^2	Laplace operator
ε	infiltration rate in the phreatic aquifer [length/time]
Λ	boundary of an aquifer
ϕ_r	real part of dZ_h
ϕ_i	imaginary part of dZ_h
ψ_r	real part of dZ_q
ψ_i	imaginary part of dZ_q
ω	frequency
Ω	domain of aquifer
$\int_\Lambda \cdots d\Lambda$	integral of elements at free surface of aquifer
$\iint_\Omega \cdots d\Omega$	double integral of elements in aquifer domain

REFERENCES

1. Bakr, A. A., 1976, "Stochastic Analysis of the Effect of Spatial Variations in Hydraulic Conductivity on Groundwater Flow," Ph.D. dissertation, N. Mex. Inst. Of Mining and Technol., Socorro.
2. Bakr, A. A., Gelhar, L. W., Gutjahr, A. L., and MacMillan, J. R., 1978, "Stochastic Analysis of Variability in Subsurface Flows, 1, Comparison of One- and Three- Dimensional Flows," *Water Resources Research*, Vol. 14, No. 2, pp. 263-271.
3. Bear, J., 1972, *Dynamics of Fluids in Porous Media*, Elsevier Science, N. Y.
4. Gelhar, L. W., 1974, "Stochastic Analysis of Phreatic Aquifers," *Water Resources Research*, Vol. 10, No. 3, pp. 539-545.
5. Gelhar, L. W., 1976, "Effects of Hydraulic Conductivity Variations on Groundwater Flows," *Proceedings of Second International IAHR Symposium on Stochastic Hydraulics*, International Association of Hydraulic Research, Lund, Sweden.
6. Gelhar, L. W., 1986, "Stochastic Subsurface

Hydrology from Theory to Applications," *Water Resources Research*, Vol. 22, No. 9, pp. 135S-145S.
7. Gelhar, L. W., 1993, *Stochastic Subsurface Hydrology*, Prentice Hall, N. J.
8. Gutjahar, A. L., Gelhar, L. W., Bakr, A. A., and MacMillan, J. R., 1978, "Stochastic Analysis of Spatial Variability in Subsurface Flows, 2, Evaluation and Application," *Water Resources Research*, Vol. 14, No. 5, pp. 953-959.
9. Hantush, Mohamed M., and Marino, Miguel A., 1994, "Continuous Time Stochastic Analysis of Groundwater Flow in Heterogeneous Aquifers," *Water Resources Research*, Vol. 31, No. 3, pp. 565-575.
10. Marschall, P., and Barczewski, B., 1989, "The Theory of Slug Tests in the Frequency Domain," *Water Resources Research*, Vol. 25, No. 11, pp. 2388-2396.
11. Zienkiewicz, O.C., and Taylor, R. L., 1989, *The Finite Element Method, Fourth Edition, Volume 1, Basic Formulation and Linear Problems*, McGraw-Hill Book Co., Singapore, pp. 290-318.

Manuscript Received: Nov. 10, 2000
Revision Received: June 23, 2001
and Accepted: July 04, 2001

未受壓含水層中引致性壓力變化之傳輸

溫志超　黃國勳

國立雲林科技大學水土資源及防災科技研究中心

呂鴻光

行政院環保署廢棄物管理處

摘　要

本研究建立數值方法模擬地下水中水頭擾動的行爲。文章中同時提出解析解與數值解。本文也同時檢查飽和土壤儲水係數及孔隙率對地下水水頭擾動的影響。由研究發現，一維地下水層中，受擾動地下水水頭的傳遞快慢受飽和土壤儲水係數及有效孔隙率的影響。此外，由地下水水頭擾動量傳遞特性發現，當傳遞距離超過 0.75 倍全長，此時傳遞之受擾動地下水水頭愈趨近於漸近行爲。

關鍵詞：水頭擾動，傳遞，含水層。